

Sawtooth behavior in a burning plasma experiment

Holger Reimerdes*

Columbia University, New York, NY

1. Introduction

Sawtooth oscillations are periodic relaxation oscillations of central temperature, density and other plasma parameters, which are common to most standard tokamak scenarios. A slow rise principally of temperature, during the sawtooth ramp is followed by the onset of the $m/n=1/1$ internal kink mode causing a rapid drop, the so-called sawtooth crash. During this crash a reconnection process results in the drop of the central temperature. The corresponding outward transport of energy defines an inversion radius ρ_{inv} , which separates the central region where energy is lost, from an outer region where energy is deposited. The inversion radius is closely related to the $q=1$ surface. The investigation of sawteeth has concentrated on three separate aspects: firstly, on the instability triggering the sawtooth crash, secondly, on the relaxation process leading to the rapid outward transport, and finally, on the transport of particles and energy as well as current diffusion during the sawtooth ramp.

Since the repetitive flattening of the central temperature profile over a significant fraction of the minor radius can have an important effect on a burning plasma, the processes that determine the sawtooth cycle are analyzed for the three proposed burning plasma experiments (BPXs) FIRE, Ignitor and ITER. Estimates of sawtooth stability parameters lead to a qualitative prediction of the sawtooth behavior in the proposed experiments. The uncertainties in the predictions are highlighted and the potential impact of sawtooth crashes in a BPX is discussed.

2. The sawtooth trigger

A comprehensive model of the sawtooth trigger has been developed by Porcelli et al. [Porcelli 96]. In the following the notation and normalization adopted in [Porcelli 96] will be used. The potential energy is normalized according to

$$\delta\hat{\mathcal{W}} \equiv -\frac{4\delta W}{s_1\xi^2\varepsilon_1^2RB^2}, \quad (1)$$

with s being the magnetic shear, ξ the radial displacement and ε the inverse aspect ratio. The subscript 1 denotes the values at the $q=1$ surface. This definition of $\delta\hat{\mathcal{W}}$ yields $\delta\hat{\mathcal{W}} = \gamma\tau_A$, where γ is the growth rate of the mode. The hat notation will be dropped.

The macroscopic drive of the mode is described by an effective potential energy functional δW , which includes the ideal MHD potential energy δW_{MHD} [Bussac 75], the

* Email: reimerdes@fusion.gat.com

stabilizing effect of thermal trapped ions δW_{KO} , and kinetic effects related to high energy particles (fusion alphas, ICRF accelerated ions and beam ions) δW_{fast} [Coppi 90],

$$\delta W = \delta W_{MHD} + \delta W_{KO} + \delta W_{fast}. \quad (2)$$

According to this model a sawtooth crash is triggered when the diamagnetic rotation cannot stabilize the mode growth,

$$-\delta W > 0.5\omega_{*i}\tau_A. \quad (3)$$

Since the structure of this mode is very similar to the structure of the ideal mode it is referred to as ideal internal kink. When the ideal mode is stable and the potential energy close to marginal stability,

$$|\delta W| < \max\{0.5\omega_{*i}\tau_A, \rho_i/a\}, \quad (4)$$

with ρ_i being the thermal ion Larmor radius, microscopic effects in the vicinity of the $q=1$ surface determine the mode dynamics. Reconnection can occur when the characteristic growth rate of the resistive internal kink exceeds the diamagnetic drift frequency,

$$\gamma_\rho > (\omega_{*e}\omega_{*i})^{1/2}. \quad (5)$$

Since the growth rate γ_ρ depends on s_1 , this triggering condition can be expressed by a criterion for the local shear at the $q=1$ surface,

$$s_1 > s_{crit}. \quad (6)$$

The regimes of the ideal and the resistive internal kink triggering the sawtooth crash can lead to very different mode dynamics. Since the ideal MHD potential energy is associated with a critical pressure gradient, a sawtooth period determined by the ideal internal kink mode scales with the energy confinement time. If resistive effects are important the sawtooth period depends largely on the current profile evolution and scales with the resistive diffusion time scale. Such a change of sawtooth dynamics, which depend on the relevant trigger regime, has been experimentally observed [Reimerdes 00]. When the stabilizing effect of δW is sufficiently strong,

$$\delta W > \max\{0.5\omega_{*i}\tau_A, \rho_i/a\}, \quad (7)$$

the mode changes its nature from a resistive internal kink to a drift-tearing mode [Cowley 86], which is assumed to be too localized near the $q=1$ surface to trigger a sawtooth crash.

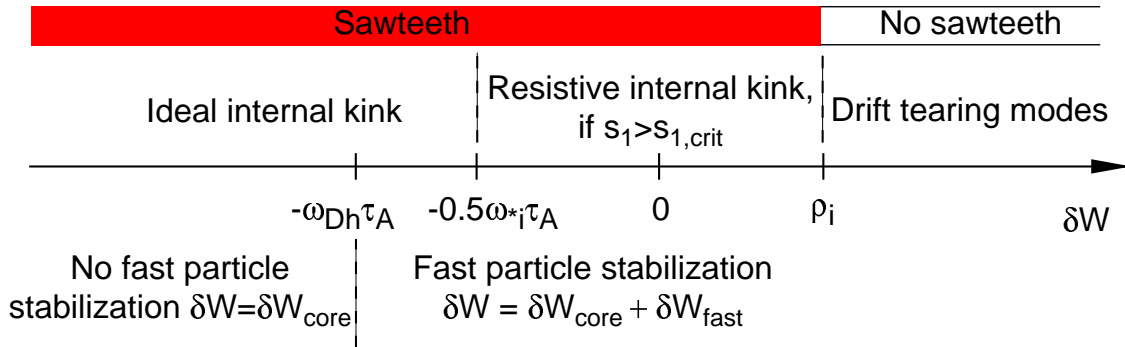


Figure 1 Schematic of the relevant sawtooth trigger according to the Porcelli sawtooth model [Porcelli 96] as a function of the potential energy functional δW .

Ideal internal kink ($m=1$)

The ideal internal kink becomes unstable once central pressure gradients are sufficiently large. An analytic expansion of the energy functional of the ideal internal kink in a circular torus was first calculated by Bussac [Bussac 75],

$$\delta W_{Bussac} = -3(1-q_0) \left(\beta_{p1}^2 - \frac{13}{144} \right), \quad (8)$$

where $\beta_{p1} \equiv (\langle p \rangle_1 - p_1) / (B_p^2(r_1) / 2\mu_0)$ is used as a measure of the pressure gradient on the $q=1$ surface. In addition to the bulk plasma the pressure p also includes the α -pressure. The expansion of the energy functional (8) assumes that $\Delta q \equiv (1-q_0) \sim e_1^2$ is a small parameter. The stability of the ideal internal kink mode is greatly altered by plasma shaping. Plasma elongation κ is predicted to reduce its stability [Wahlberg 98], while triangularity δ can reduce the destabilizing effect of elongation [Eriksson 02]. The predicted shape dependence is in qualitative agreement with experiments [Reimerdes 00]. The analytic expression, however, is not sufficient for a quantitative prediction of δW in an experiment. Firstly, Δq can become too large to be treated as a small parameter, which leads to a reduction of stability as the inversion radius increases. Secondly, the experimental boundary does not correspond to the fixed boundary assumed in the analytic expansions leading to a further reduction of the stability [Jardin 02]. An accurate expression for the ideal MHD energy potential of the ideal internal kink mode has to be compared to numeric full ideal MHD calculations.

Fast particle stabilization of sawteeth

In a burning plasma experiment the effect of fast alpha particles are expected to be important. The stabilizing influence of fast particles is a consequence of the conservation of the third adiabatic invariant, i.e. the magnetic flux linked through the fast trapped ion precessional drift orbits [Coppi 90, Porcelli 91]. This constraint becomes relevant when particles complete more than one orbit within the characteristic time scale of the magnetic perturbation,

$$c_h \omega_D \tau_A > -\delta W_{core}, \quad (9)$$

where c_h is of order unity, ω_D the precession frequency and $\delta W_{core} = \delta W_{MHD} + \delta W_{KO}$ the potential energy of the plasma core. In addition to the D-T fusion born alpha particles ($E=3.52\text{MeV}$) fast particles can be generated by neutral beam heating ($E=50\text{-}150\text{KeV}$), and Ion Cyclotron Resonance Heating (ICRH) ($E=100\text{KeV-}1\text{MeV}$). Analytic theory provides an expression for the stabilizing effect of fast particles, which is additive to the potential energy [Coppi 90],

$$\delta W_{fast} = c_f \epsilon_1^{3/2} \beta_{p\alpha}^* / s_1, \quad (10)$$

where $\beta_{p\alpha}^*$ is defined in [Porcelli 96] and the factor c_f depends on the ratio between the mode frequency and the fast particle precession frequency. In the limit $\gamma_{core} \ll \omega_D$, c_f reduces to unity.

The stabilizing effect of fast particles is well documented in experiments. In JET fast particles, in particular those arising from ICRH, lead to a substantial increase of the sawtooth period [Campbell 88]. The sawtooth period/sawtooth-free period can last up to several seconds. The stabilizing effect disappears after the switch-off of the ICRH power

with a time-delay, which corresponds to the fast ion slowing down time. Similar observations are made on other experiments. Fast particle effects were also seen in the JET DTE1 experiments with different D-T mixtures, where an increase of the sawtooth period with the mean ion-mass was observed. Since the beam slowing-down time increases with the tritium concentration, the increased beam population was identified as the main effect, causing the sawtooth stabilization [Nave 02]. It was also shown that beam ions with energies up to 140MeV alone can be sufficiently energetic to have a stabilizing effect [Angioni 02 a].

Assessment of the internal kink stability in FIRE, Ignitor and ITER

A zero-dimensional analysis of the sawtooth stability in the three proposed devices is carried out. The stability parameters are calculated from typical machine parameters listed in the appendix. The calculation assumes a $q=1$ surface at mid-radius and a local shear of $s_1=0.5$.

In order to evaluate the relevance of fast particle stabilization in a BPX, an order of magnitude estimate of the ideal internal kink growth rate is compared with the projected α -particle precession frequency $\omega_{D\alpha} \sim E_\alpha / (BRr_1)$. Since $\delta_1 \sim 0.5\varepsilon_1$, the leading order term of δW vanishes [(2c) in Eriksson 02], and $-\delta W_{MHD}$ is estimated to be of the order of $\varepsilon_1^2 \beta_{p,1}^2$. The contribution of the α -particles to the total pressure depends on the α -particle slowing down time τ_α . A power balance estimate for ignition results in $\beta_{p\alpha} \sim (\tau_\alpha / \tau_E) \beta_{p,core}$. The ratio of $\beta_{p,1}$ to β_p has been evaluated for parabolic pressure- and q -profiles and increases with increasing pressure profile peaking $p_0 / \langle p \rangle$. Hence, this ratio is largest for Ignitor (Table 1), which is projected to operate with $p_0 / \langle p \rangle \sim 4$ (Table 2 in appendix).

	FIRE	Ignitor	ITER
τ_A	0.61 μ s	0.40 μ s	1.5 μ s
$\tau_\alpha \sim T_e^{3/2} / n_e$	0.14 s	0.040 s	1.07 s
$\omega_{D\alpha}$	$9.4 \times 10^4 \text{s}^{-1}$	$1.5 \times 10^5 \text{s}^{-1}$	$1.8 \times 10^4 \text{s}^{-1}$
$\omega_{D\alpha} \tau_A$	0.057	0.060	0.027
τ_α / τ_E	0.14	0.064	0.29
$\beta_{p\alpha} \sim (\tau_\alpha / \tau_E) \beta_{p,core}$	0.14	0.013	0.19
$\beta_{p,1} / \beta_p$	0.67	0.90	0.67
$-\delta W_{MHD} \sim \varepsilon_1^2 \beta_{p,1}^2$	0.021	0.0021	0.015
ρ_1 / r_1	4.9×10^{-3}	3.9×10^{-3}	2.8×10^{-3}
δW_{fast}	0.015	0.0027	0.025

Table 1 Estimates of sawtooth stability parameters in FIRE, Ignitor and ITER.

The precession frequency of the α -particles is approximately 3 times larger than the estimated growth rate of the internal kink mode excluding fast particle effects in FIRE and Ignitor and 2 times larger than the estimated growth rate in ITER (Table 1). Fast particles should, therefore, have a stabilizing effect in all three devices.

The potential of the fast particle stabilization (10) increases with the α -particle beta $\beta_{p\alpha}^*$. The averaging of the α -pressure gradient over the region inside the $q=1$ surface, used in the definition of $\beta_{p\alpha}^*$, is approximated by $\beta_{p\alpha}^* \sim \beta_{p\alpha,1}$. A comparison of $-\delta W_{MHD}$ and δW_{fast} (Table 1) shows that the stabilizing potential for all three devices is of the same order of magnitude than the estimate of the ideal MHD unstable potential. In the case of Ignitor and ITER δW_{fast} exceeds $-\delta W_{MHD}$ by $\sim 50\%$, whereas in FIRE it is $\sim 30\%$ smaller. Since δW_{MHD} and δW_{fast} have a different dependence on s_1 , it is likely that δW_{fast} of a relaxed profile ($s_1 \ll 1$) is sufficiently large to stabilize the internal kink mode. Then the sawtooth period is determined by flux diffusion and the corresponding expansion of the $q=1$ surface. These estimates of the sawtooth stability are in good agreement with detailed calculation using the TSC code coupled to the Porcelli sawtooth model [Jardin 02].

Simulations of sawteeth in ITER-EDA using the PRETOR transport code showed clearly that the ideal MHD potential energy is not a good indication of internal kink stability in ITER, as kinetic contributions to δW dominate [Porcelli 96]. In an ignited scenario fast particles are predicted to stabilize the internal kink as long as the inversion radius does not exceed 50% of the minor radius. In these simulations sawteeth are triggered by the resistive internal kink mode as the $q=1$ radius expands. The obtained sawteeth resemble the ‘monster sawteeth’ in JET [Campbell 88].

3. The sawtooth crash

The most prominent relaxation model is Kadomtsev’s complete reconnection model [Kadomtsev 75]. According to this model the $m=1$ island grows until it fills the entire plasma center out to the mixing radius leading to a safety factor of unity on axis and above elsewhere. This is, however, not always consistent with experiments where safety factors well below unity are frequently observed after the sawtooth crash. The observation of the formation of shoulders at the $q=1$ surface [Soltwisch 86] supports the ideal of partial reconnection up to some critical island width. Even the relaxation of the temperature profile without any reconnection is thought to be possible [Coppi 02]. Simulations have shown that the amount of reconnected flux can greatly influence the sawtooth period with less reconnection leading to shorter sawtooth periods [Porcelli 96]. Recent simulation of beam ion stabilized sawteeth in low- β JET discharges achieved good agreement assuming full reconnection [Angioni 02 a].

4. Transport during the sawtooth ramp

The evolution of the relaxed profiles to a sawtooth-unstable state is determined by the relaxed profiles, the central heating source, energy transport and flux diffusion. Since the energy confinement time is smaller than the current diffusion time the pressure profile can saturate during long sawtooth periods while the current profile still evolves (increase of r_{inv} and decrease of q_0). Recent DIII-D experiments showed that the current profile can also saturate with values of q_0 above unity, when an $m/n=3/2$ tearing mode is present which effectively prevents flux from diffusing further inward [Wade 02].

5. Effect of sawteeth on profiles and performance

Since fast particle effects will play an important role in the proposed experiments, it is likely that the sawtooth period is determined by flux diffusion and the corresponding expansion of the $q=1$ surface. The sawtooth period is, therefore, expected to be larger than the energy confinement time resulting in large sawtooth crashes and a flattening of the temperature profile over a large fraction of the minor radius, similar to JET “monster sawteeth” [Campbell 88].

Confinement

The flattening of the temperature profile leads to a redistribution of energy but only a small energy loss (<5%), which can be seen in Fig. 2 (JET pulse 42677). The effect on the fusion yield is somewhat larger and increases with decreasing central temperature due to the temperature dependence of the D-T fusion cross-section. The drop of the fusion yield is, therefore, expected to be more severe in Ignitor and less in ITER. This is consistent with detailed transport calculations [Jardin 02].

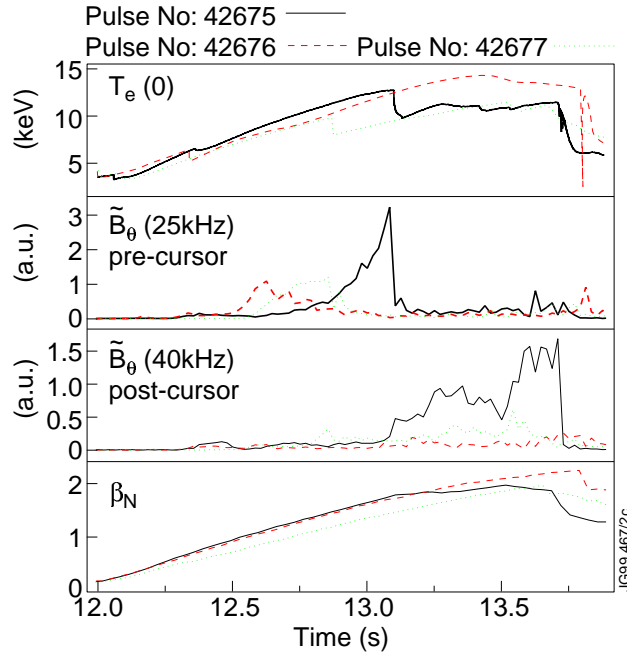


Figure 2: JET ELM-free D-T discharges ($q_{95} = 3.5$, $\eta_r = 50\%$) where fast particle stabilization leads to monster sawteeth. The discharges differ in the gas-fuelling rate and ICRH power. The sawtooth crash can trigger $n>2$ modes, which are probably NTMs [Nave 02].

α -particles

There is an uncertainty about the behavior of fast α -particles, which will not necessarily redistribute in the same way than the thermal plasma. Measurements on D-T plasmas in TFTR show a broadening of the α -density profile after a sawtooth crash [Petrov 95]. The sawtooth crash redistributes fast α -particles radially outwards closer to regions where they could be affected by stochastic ripple loss. Although no significant ripple loss was observed in the TFTR experiments, a larger inversion radius could enhance these losses

[Zweiben 00]. The potential loss of the fast particles would have the largest impact in ITER, which has the largest ratio of slowing-down time to energy confinement time, $\tau_\alpha/\tau_E \sim 0.3$ and, hence, the largest fast α -population (Table 1).

Impurities

Sawteeth can also be beneficial by preventing the accumulation of impurities in the plasma center. This has been demonstrated in recent JET RI experiments with Argon, where an accumulation of impurities in the core was always observed in non-sawtooth discharges. The impurity accumulation was prevented, in plasmas where sawteeth were re-introduced by controlling $q(0)$ with ICRH [Nave 01].

Coupling to other MHD

A main concern arises from the potential coupling of the sawtooth to other MHD modes. Sawtooth crashes can couple to ELMs or trigger $m > 1$ modes (e.g. in JET pulse 42675, Fig. 2), such as neoclassical tearing modes, which are predicted to be meta-stable in FIRE and ITER. The coupling of a monster sawtooth to a large ELM after an ELM-free phase terminated the high performance phase in JET hot-ion H-modes, while just having a modest effect on energy confinement [Nave 95]. In JET DTE1 experiments delaying sawteeth was found to be crucial in the quest for high fusion power. The highest fusion power was obtained in a discharge with $q_{95} = 3.5$, where large sawteeth were delayed [Nave 02]. A coupling of sawteeth and ELMs is also observed in ELMy JET discharges at high β ($\beta_N > 0.5$) [Alper 94]. In these discharges β and the neutron rate recover after the crash and are only limited by the occurrence of the next sawtooth/ELM event. The triggering of an NTM by a sawtooth crash is observed in many experiments (e.g. ASDEX-U and DIII-D [Gude 99, La Haye 00]) and has an important effect on performance and energy confinement. In JET larger sawtooth crashes are observed to trigger NTMs at lower values of β_N (Fig. 3) [Sauter 02].

6. Sawtooth control

A mean to control the occurrence of sawteeth is very desirable, since it can prevent a possible accumulation of impurities in the plasma center and increase the β_N threshold for the onset of NTMs. The sawtooth stability can be altered by applying localized heating and/or current drive. This has been demonstrated in several experiments, such as TCV and ASDEX-U, using localized ECRH/ECCD in the vicinity of the $q=1$ surface [Angioni 01, Mueck 02]. Small amounts of ECCD (4% of the local current density) are deemed sufficient to alter the sawtooth period in TCV by more than 50% [Angioni 02 b]. The increase of the NTM β_N threshold has been successfully demonstrated in JET using localized ICRH/ICCD just outside the sawtooth inversion radius, which decreased the sawtooth period and allowed one to avoid triggering an NTM [Sauter 02].

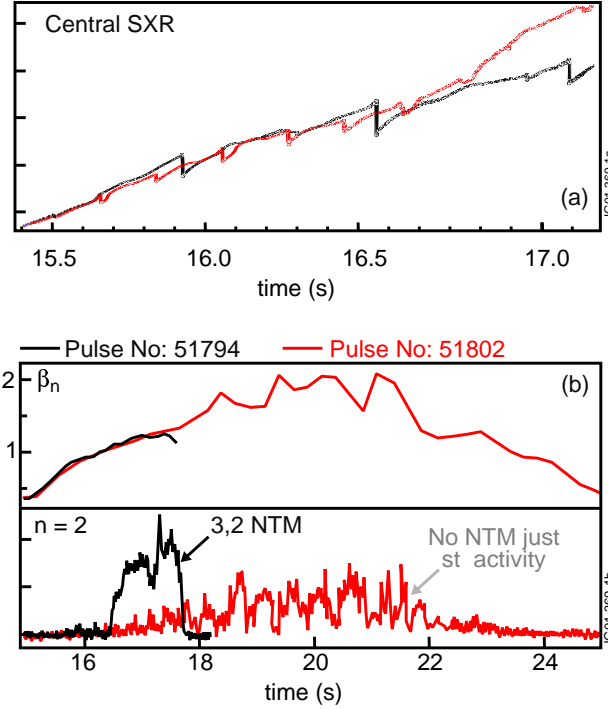


Figure 3 Similar JET discharges with different sawtooth behavior. In the discharge with larger sawtooth periods, the crash at 16.4 s (a) triggers a neoclassical tearing mode (b) at a low value of β_N . The discharge with more frequent but smaller sawteeth achieves a higher value of β_N without triggering an NTM [Sauter 02].

7. Conclusion

All three devices, FIRE, Ignitor and ITER, are subject to fast particle stabilization of the internal kink mode. While Ignitor has the least unstable ideal MHD potential, which is in line with the low- β_p Ignitor concept, it also has the smallest potential of fast particle stabilization. In all three devices the ideal MHD potential, δW_{MHD} , is compensated by a fast particle potential, δW_{fast} , in the respective same order of magnitude. Thus, δW_{MHD} alone is not a good indicator of the sawtooth stability. In spite of uncertainties in the determination of the ideal MHD potential, the amount of reconnection and the transport during the sawtooth ramp, the sawtooth stability is, therefore, likely limited by flux diffusion and the corresponding expansion of the $q=1$ surface. This leads to a sawtooth period, τ_{saw} , which is longer than the energy confinement time, τ_E , and large sawteeth, which will resemble JET giant sawteeth. In order to increase the confidence in the prediction it would be desirable to model sawteeth in high- β_p discharges and address the uncertainty about the amount of reconnecting flux at high β . While the sawtooth crash itself causes only a modest confinement degradation, especially, when $\tau_{saw} \gg \tau_E$, the coupling to other MHD, in particular NTMs, is a major concern in FIRE and ITER. The ability to control the size of the sawtooth crash should, therefore, become an important tool in FIRE and ITER. Schemes, where localized current drive (e.g. ECCD, ICCD) in the vicinity of the $q=1$ surface increases γ_{MHD} and/or causes a loss of fast particle stabilization, can allow a control of the sawtooth period.

Acknowledgements

Thanks to F. Nave and O. Sauter for helpful comments and providing material. The author also acknowledges very helpful discussions with D. Campbell, P. Detragiache, S. Jardin, T. Strait and L. Sugiyama as well as within the Snowmass MHD working group.

Appendix

Device	FIRE	Ignitor	ITER
$A(m)/R(m)$	0.6/2.14	0.47/1.32	2.0/6.2
κ	1.8	1.8	1.8
$B(T)$	10	13	5.3
$I_p(MA)$	7.7	11	15
$n(10^{20}m^{-3})$	5.0	9.5	1.0
$T_{e0}(KeV)$	15	10	20
$p_\sigma/\langle p \rangle$	2.5	4.0	2.5
$\beta_{p,core}$	1.0	0.20	0.65
$\tau_E(s)$	1.0	0.62	3.7

Table 2: Characteristic parameters for the proposed burning plasma experiments.

References

- [Porcelli 01] F Porcelli et al., *Plasma Phys. Control. Fusion* **38** (1996) 2163.
 [Bussac 75] M N Bussac et al., *Phys. Rev. Lett.* **35** 1638
 [Coppi 90] B Coppi et al, *Phys. Fluids B* **2** (1990) 927.
 [Reimerdes 00] H Reimerdes et al., *Plasma Phys. Control. Fusion* **42** (2000) 629.
 [Cowley 86] S C Cowley et al., *Phys. Fluids* **29** (1986) 3230.
 [Wahlberg 98] C Wahlberg, *Phys. Plasma* **5** (1998) 1387.
 [Eriksson 02] H G Eriksson and C Wahlberg, *Phys. Plasma* **9** (2002) 1606.
 [Jardin 02] S Jardin et al, “m=1 mode: simulations”, Snowmass 2002 summary report.
 [Porcelli 91] F Porcelli, *Plasma Phys. Control. Fusion* **33** (1991) 1601.
 [Campbell 88] D J Campbell et al., *Phys. Rev. Lett.* **60** (1988) 2148.
 [Nave 02] M F F Nave et al, *Nucl. Fusion* **42** (2002) 281.
 [Angioni 02 a] C Angioni et al., *Plasma Phys. Control. Fusion* **44** (2002) 205.
 [Kadomtsev 75] B B Kadomtsev, *Sov. J. Plasma Phys.* **1** (1975) 389.
 [Soltwisch 86] H Soltwisch et al., *Plasma Phys. Contr. Fus. Res. 1986* vol I (1986) p433.
 [Coppi 02] B Coppi, private communication.
 [Wade 02] M Wade et al., 29th EPS conference (Montreux) (2002).
 [Petrov 95] M P Petrov et al, *Nucl. Fusion* **35** (1995) 1437.
 [Zweben 00] S J Zweben et al, *Nucl. Fusion* **40** (2000) 91.
 [Nave 01] M F F Nave et al., Proc of 28th EPS conference (Madeira, 2001).
 [Nave 95] M F F Nave et al., *Nucl. Fusion* **35** (1995) 409.

- [Alper 94] B. Alper et al., Proc. 21st EPS Conference on Controlled Fusion and Plasma Physics (Montpellier), Part I (1994) p.202.
- [Gude 99] A Gude et al, *Nucl. Fusion* **39** (1999) 127.
- [La Haye 00] R J La Haye et al, *Nucl. Fusion* **40** (2000) 53.
- [Angioni 01] C Angioni et al, Theory of Fusion Plasmas, Joint Varenna-Lausanne Int. Workshop (2001) p73.
- [Mueck 02] A Mueck et al, Proc of 29th EPS conference (Montreux, 2002).
- [Angioni 02 b] C Angioni et al, Proc of 29th EPS conference (Montreux, 2002).
- [Sauter 02] O Sauter et al, *Phys. Rev. Lett.* **88** (2002) 105001.